



IMAGING FEATURES OF VARIOUS CEREBELLO-PONTINE ANGLE LESIONS

Radiodiagnosis

Dr. Gorli Divya Rani

Final Year Post Graduate, Dept Of Radio-diagnosis, NRI Medical College, Andhra Pradesh, India

Dr. D. Ankamma Rao*

DMRD, DNB, Professor, Dept of radio-diagnosis, NRI Medical College, Andhra Pradesh, India *Corresponding Author

ABSTRACT

Introduction: Cerebellopontine angle (CPA) tumours usually are classified into intra-axial, extra-axial, skull base tumours. Although vestibular schwannomas and meningiomas constitute the vast majority of the cerebellopontine angle (CPA) lesions, a large variety of unusual lesions can also be encountered in the CPA.

In the present study, the CT and MRI imaging features of various cerebellopontine angle tumours are evaluated.

Material and Methods: All patients with clinical suspicion of cerebellopontine (CP) angle tumours are subjected to scan on the 1.5T MR imaging system. Special sequences such as DWI, MR spectroscopy were performed.

Results: Acoustic schwannomas, which are also known as Vestibular schwannomas, and meningiomas are the two most frequent lesions and account for approximately 85%-90% of all CPA tumours. The other 10%-15% includes a large variety of lesions that will be recognised more frequently because of the remarkable sensitivity and accuracy of magnetic resonance imaging in the evaluation of a CPA syndrome. Computerised tomography (CT) and magnetic resonance imaging (MRI) are the primary modalities for diagnosis of cerebellopontine lesions. MRI is considered superior in differentiating the different types of Cerebellopontine angle (CPA) masses. Knowledge of typical signal characteristics and more specific features such as a hemispheric or ice-cream cone shape, a dural tail, adjacent hyperostosis, extension into one or more skull base foramina, and enlargement of the internal auditory canal (IAC) helps in limiting the differentials considered. Recent advanced MRI techniques that include diffusion-weighted imaging (DWI), MR spectroscopy, and MR perfusion can help provide a more specific diagnosis.

Conclusion: MRI is the most sensitive noninvasive modality to characterise CP angle tumours. MRI identifies the exact location and extension of the lesions based on their signal characteristics and contrast enhancement pattern.

KEYWORDS

Cerebellopontine Angle Tumor, Schwannoma, Meningioma

INTRODUCTION

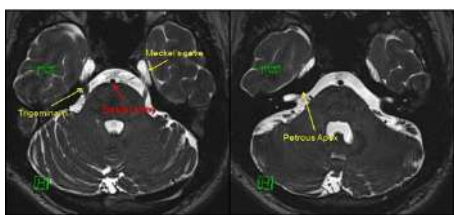
Acoustic schwannomas, which are also known as Vestibular schwannomas, and meningiomas are the two most frequent lesions and account for approximately 85%-90% of all CPA tumours.

The other 10%-15% includes a large variety of lesions that will be recognised more frequently because of the remarkable sensitivity and accuracy of magnetic resonance imaging in the evaluation of a CPA syndrome.

Normal anatomy of Cerebellopontine angle (CPA)

The Cerebellopontine Angle (CPA) is the space-bound by the cerebellum, pons, and temporal bone. Space is bound anteriorly by the posterior surface of the temporal bone and posteriorly by the anterior surface of the cerebellum. The inferior olive and the superior boundary form the medial boundary by the inferior border of the pons and cerebellar peduncle. The cerebellar tonsil forms the inferior border (1). It contains the short intracranial courses of the fifth, seventh, and eighth cranial nerves. The seventh and eighth cranial nerves course superiorly and laterally toward the IAC within this space. Superiorly, the fifth nerve is visible, with the ninth, tenth, and eleventh nerves located inferiorly. The seventh and eighth nerves are encased in the glial tissue throughout their intracranial course Schwann cells surround these nerves beginning in the IAC, near the porus (Fig 1). The Glial-Schwann junction is also known as Obersteiner- Redlich zone. The vestibular ganglion (Scarpa's ganglion) is located near the mid-portion of the IAC. (1) The division of the eighth nerve into vestibular and cochlear segments occurs in the subarachnoid space or in the medial segment of the IAC. Vestibular segment divides into superior and inferior vestibular nerves, which occupy the posterior half of the IAC.

Figure 1



The tumours can derive from various anatomical structures, including primary origin from internal auditory meatus, pontocerebellar cistern, and the lateral recess of the fourth ventricle, temporal bone, brain stem, or cerebellar tissue. (2-4) Clinical presentation of the CPA tumours is variable, and it depends upon the size and location of the tumour. It can be asymptomatic in early-stage or it can give vertigo, tinnitus, or hearing loss. Vascular compression of the vestibulocochlear nerve also causes vertigo and tinnitus. Large CPA lesions may compress the pons, the ipsilateral cerebellar hemisphere, the trigeminal nerve anteriorly and superiorly, and the IX, X, and XI nerves posteriorly.

Computerised tomography (CT) and Magnetic Resonance Imaging (MRI) are the primary modalities for the diagnosis of cerebellopontine lesions. MRI is considered superior in differentiating the different types of CPA masses.

Knowledge of typical signal characteristics and more specific features such as ice-cream cone shape, a dural tail, adjacent hyperostosis, extension into foramina of the skull base and enlargement of the internal auditory canal (IAC) helps in limiting the differentials considered.

Recent advanced MRI techniques that include diffusion-weighted imaging (DWI), MR spectroscopy, and MR perfusion can help provide a more specific diagnosis.

The Cerebello-pontine angle lesions can be classified based on their contrast enhancement as enhancing or non enhancing lesions. In enhancing lesions, they are classified based on the location as Extra-axial, Intra-axial, Skull Base tumours. In non-enhancing lesions they are classified base on the signal intensity on T1 and T2.

MATERIALS AND METHODS

In our study, we analysed 50 patients with clinical suspicion of cerebellopontine angle lesions and CT & MRI were performed based on imaging requirements. T2-W image axial, sagittal and coronal planes, T1W images axial and sagittal plane, and constructive interference in steady-state (CISS) axial images were taken, post gadolinium T1WI in the axial, coronal and sagittal plane were also obtained whenever needed.

Total number of cases in our study: 50

Place of study: NRI Medical College and General Hospital

Duration of study: 2017 to 2019

RESULTS

A total of 50 patients were included in the study. Out of which extra-axial lesions are the most common lesions of the cerebellopontine angle.

In our study, there were 20 cases of Schwannoma, 8 cases of Meningioma, 3 cases of Epidermoid cyst, 2 cases of Arachnoid cyst, 2 cases of Metastasis, 2 cases of Aneurysms, 2 cases of Chordoma, 1 case of each Glioma, Choroid plexus Papilloma, Pseudotumour, Tuberculosis, Complication of Mastoiditis, Lipoma, Neuroenteric cyst, Paranglioma, Melanoma, Cholesterol granuloma, Perineural spread of Carcinoma Nasopharynx into the cerebellopontine angle.

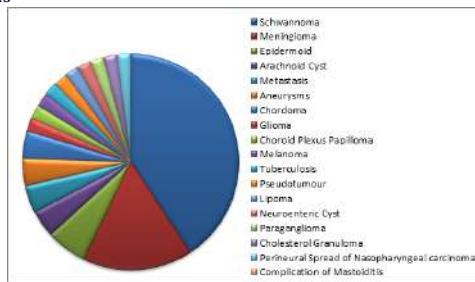
Most common extra-axial tumours of CPA are Acoustic schwannomas; second most common tumours are meningiomas. Epidermoid and arachnoid cysts are less common CPA tumours.

Intra-axial tumors at Cerebello-pontine angle (CPA) are Glioma, Metastasis, Choroid plexus Papilloma.

Skull base tumours are Chordoma and Parangliomas.

Non-enhancing lesions include Lipoma, Neuroenteric cyst, Cholesterol granuloma, Epidermoid cyst and Arachnoid cyst.

Pie Chart depicting various types of Cerebello-Pontine Angle lesions



DISCUSSION

Total of 50 cases were included in our study.

The Cerebello-pontine angle lesions can be classified based on their contrast enhancement as enhancing or non enhancing lesions.

In enhancing lesions, they are classified based on the location as Extra-axial, Intra-axial, Skull Base tumours.

In non-enhancing lesions, they are classified based on the signal intensity on T1 and T2.

Enhancing lesions:

Vestibular Schwannoma:

Schwannoma is a benign (WHO grade I) encapsulated tumour that arises from the Schwann cells of the nerve sheaths of cranial and spinal nerves. (5). They represent 80-85% of the CPA tumours. (6) Intracranial schwannomas occur in all the age groups, with a peak incidence in the 4th to 7th decades of life. (6,7) There is a sex predilection with a female-to-male ratio of 2:1.(8,9) The most common site of Schwannoma is Scarpa's ganglion, where the highest concentration of Schwann cells are found. The symptom depends upon the size and location of the tumour. Bilateral vestibular schwannomas when found, strongly suggest the presence of neurofibromatosis type 2 (NF-2), a neurocutaneous disorder associated with a mutation on the long arm of chromosome 22. (10) The occurrence of bilateral vestibular schwannomas is almost considered the pathognomonic of this disorder, which has also been termed multiple inherited schwannomas, meningiomas, and ependymomas. (11) MRI is the excellent modality to detected small tumours, especially within the IAC, because of the lack of bone-induced artefact and the multidimensional capability of this modality. Tumours <5 mm in diameter can be reliably identified on CISS images, appearing as homogeneously mildly hypo- or iso-intense (to adjacent brain) ovoid or tubular intracanalicular masses,

hypointense on T1WI with intense homogeneous contrast-enhancement(3,9,12,13). On T2W images, they appear mildly to markedly hyperintense and may be obscured by the similarity in the signal to that of the surrounding cerebrospinal fluid (CSF). In larger tumours, intratumoral degenerative changes may result in an increase in heterogeneity of signal. The differential diagnosis is meningioma and epidermoid tumour.(3,12,13) Meningioma involving the dura of the posterior margin of the petrous temporal bone can project posteriorly into the CPA and simulate a vestibular schwannoma.

Meningioma

Meningiomas are solid, well-circumscribed, and slow-growing tumours that are composed of neoplastic meningotheial cells originating from the arachnoid layer of the meninges with a broad attachment to the adjacent dura. Meningiomas account for about 30% of all primary brain tumours with an annual incidence of about 4.5/100,000 individuals. (14) Meningiomas are the second most frequent CPA tumour, which constitutes 10-15% cases. (15) They occur with a peak incidence in the 5th to 7th decades of life. (16)Meningiomas show female predominance, with a female-to-male ratio of at least 2:1. (15) However, meningiomas associated with hereditary tumour syndromes such as NF-2 generally occur in younger patients and do not demonstrate any gender preference. (16)The WHO classified meningiomas into the following three grades: Benign (Grade I), atypical (Grade II), and anaplastic or malignant (Grade III). The grading has been done based on histological markers, which include the presence and number of mitotic figures, overall cellularity, nuclear prominence, nuclear to cytoplasmic ratio and the presence of necrosis. (17) Though the majority of meningiomas are benign Grade I tumours, 23-24% of the tumours are atypical (Grade II) and 1-3% are found to be anaplastic (Grade III) under the new WHO classification system. (18, 19) Common sites are in the frontal and parietal convexities and in the parasagittal region (in close relation with the falx cerebri). (16) Multiple meningiomas are commonly associated with NF-2. Invasion of the dura and encasement or invasion of the nearby dural venous sinuses is common. (16) On CT, meningiomas appear hyperdense, approximately 20% show calcification and after the intravenous administration of contrast medium, meningiomas typically show homogeneous contrast-enhancement (an increase of 40-50 HU or more). (20) On noncontrast MRI, the majority of meningiomas have a homogeneous appearance similar to that seen on CT; it shows a typical broad base at the meningeal origin and hemispheric shape on the opposite side. On T1WIs, they appear iso- to hypo-intense to the adjacent cerebral cortex. On T2WIs, about 50% are mildly hyperintense relative to adjacent gray matter and 50% are isointense to the cortex (20). It is hypointense on CISS sequence obliterating the vestibulocochlear nerve. Meningiomas show homogenous enhancement on post contrast T1WI. Indistinct irregular tumour margins, a mushroom-like extension of opacified tumour well away from the main ovoid tumour mass, and prominent venous drainage centrally from the tumour are CT and MRI signs that may suggest an aggressive anaplastic or malignant meningioma invading the brain. (21) MRI enables more accurate localisation and evaluation of these tumours. A thickened tapered extension of the contrast-enhancing dura is commonly identified at the margins of the tumour. Because a major prognostic factor in the recurrence of meningiomas after surgery is the extent of tumour resection, the careful assessment must be made of pre- and post-operative contrast MR images for the presence of a dural tail. (16) MR spectroscopy provides additional information to narrow down the differential diagnosis of tumours by neuroimaging is difficult. The most common proton spectrum found in meningiomas is a high Cho peak with low or absent NAA and creatine and variable amounts of lactate. A high ratio of alanine to creatine has been found in meningiomas because of the high alanine and low creatine content, and this is a relatively specific finding for meningioma.

Metastases

Intracranial metastases are ubiquitous. They may be extra-axial and mimic a meningioma or a schwannoma in the CPA or be intra-axial, exactly located in front of the IAC, often surrounded by peritumoral oedema. Multiple lesions or history of known cancer will lead to the diagnosis. Additionally, advanced MR techniques are helpful and demonstrate mean rCBV ratios lower than high-grade gliomas and higher ADC values than the enhancing portion of high-grade gliomas and abscesses (22). MR spectroscopy shows a predominant peak in lipids in metastasis, another important finding considered suggestive of the diagnosis (22).

Melanocytic Neoplasms

Melanocytes are normally present in the intracranial leptomeninges, usually in the posterior cerebral fossa (6), and can give rise to benign (meningeal melanocytoma) or malignant (malignant melanoma) tumours. However, metastatic malignant melanomas greatly outnumber primary melanocytic neoplasms (6). At CT, primary melanocytic lesions appear as well-circumscribed, isoattenuating to hyperattenuating extra-axial tumours with homogeneous enhancement. Even if there is no hyperostosis, they can mimic a meningioma (6). MR imaging demonstrates variable signal intensity on T1 and T2-weighted images in proportion to the amount of melanin within the tumour (6). Therefore, melanocytic neoplasms are isointense or hyperintense to adjacent normal brain tissue on T1-weighted images and isointense or hypointense on T2-weighted images (6). They enhance after intravenous administration of contrast material.

Other Miscellaneous Meningeal Lesions

In addition to the carcinomatous meningitis, many infectious or inflammatory diseases can have focal nodular meningeal involvement and manifest as a CPA mass. Leptomeningeal metastases from lung cancer, breast cancer, melanoma, or other neoplasms can mimic benign tumours of the CPA (6). Tuberculosis is one of the main causes of focal pachy meningeal thickening in the posterior cranial fossa, but this finding is not specific (6).

Neurosarcoidosis can also appear as a dura-based mass, like a meningioma. The lesions of neurosarcoidosis are hyperattenuating on CT scans and isointense to gray matter on T1-weighted images with homogeneous enhancement; however, the possible low signal intensity on T2-weighted images may suggest the diagnosis (6).

Vascular lesions

Such as vertebrobasilar dolichoectasia (elongation and dilatation of vertebral and basilar artery), vascular loops, and aneurysms account for 2-5% of CPA masses. They may cause symptoms by compressing cranial nerves. Vascular compression of the vestibulocochlear nerve in the CPA usually caused by a tortuous anterior inferior cerebellar artery or posterior inferior cerebellar artery or their branches. (23) Venous causes include idiopathic intracranial hypertension and dural venous thrombosis. (24) MRI with CISS images can demonstrate the vascular loop adjacent to the vestibulocochlear or facial nerve. Microvascular decompression surgery has been used to treat the cases. (25)

Aneurysm

Vertebrobasilar aneurysms and dolichoectasia account for a substantial part of non-tumoral lesions of the CPA that can lead to cranial nerves or brain stem compression (26). In this location, and even in the internal auditory canal, intracranial aneurysms may resemble vestibular schwannomas, especially on CT, because they appear as well defined round or oval lesions that intensely enhance after contrast administration (26). At MRI, aneurysms without significant internal thrombus have obvious flow voids and pulsation artefacts on all spin-echo sequences but demonstrate iso to high signal intensities and variable patterns of gadolinium uptake on T1W images when the intraluminal thrombus is present. However, the diagnosis should systematically be suspected when round/oval lesions with low to no signal intensity are seen on the T2-weighted sequence. MR angiography should then be performed to confirm the diagnosis and depict the parent artery, which could be the posterior inferior cerebellar artery, the anterior inferior cerebellar artery, the vertebral artery [26] or the basilar artery itself.

Inflammatory Pseudotumour

Inflammatory pseudotumours, also known as inflammatory myofibroblastic tumours, may involve the CNS, it most commonly produces a dural based/meningeal mass, although it may be intraparenchymal or may occasionally arise from the choroid plexus, producing a hyperdense intraventricular mass on CT imaging. On MRI, it was seen to extend into the pterygopalatine and infratemporal fossa producing a thickening of the right lateral tentorium and oedema of the right temporal lobe. Typically, inflammatory pseudotumor is hypointense on T1-weighted images and markedly hypointense on T2. The radiologic appearance of a dural-based mass may further mislead the pathologist. Intraparenchymal heterogeneously enhancing inflammatory pseudotumours may mimic a malignant brain neoplasm.

Intra-axial and intraventricular lesions

Glioma

Glial tumours of the brain stem, and especially pilocytic astrocytomas in young adults, can manifest as an asymmetric expansion of the brain stem that can rarely be pedunculated and exophytic, invading the CPA (22) and even mimicking a vestibular schwannoma by enlarging the porus acousticus (22). These tumours do not have specific imaging features in this location: they appear with T2hyperintensity, T1 hypointensity and variable enhancement depending on the glioma grade. They are usually surrounded by adjacent oedema. Diffusion and perfusion imaging of the solid portions of glial tumours also depend on their histological grade. In general, the lower the ADC value, the higher the rCBV, the higher the grade (22).

Choroid Plexus Papilloma

Most papillomas in adults are located in the posterior fossa. Although they commonly arise from the fourth ventricle, they occasionally extend into the CPA through the foramen of Lushka or primarily occur there (22). Choroid plexus papillomas, which are benign, are structurally similar to normal choroid plexus and therefore appear as calcified, vascular, enhancing masses at CT, with a possible intratumoral cyst. At MRI, papillomas appear either as homogeneous or heterogeneous cauliflower-like tumours. They are mainly iso/hypointense on T1- and T2-weighted images and strongly enhance after contrast injection unless the tumour is highly calcified. They may also contain areas of low signal intensity corresponding to calcifications, possible foci of high signal intensity due to intratumoral haemorrhage and flow voids when high flow vessels feed the tumour. Cerebral digital subtraction angiograms reveal these enlarged arteries that demonstrate a prolonged vascular blush and intratumoral arteriovenous shunting, thus potentially mimicking a hemangioblastoma in this location. Finally, hydrocephalus is often associated with choroid plexus papillomas; it may be explained in part by CSF hypersecretion by the tumour, but also by fourth ventricle obstruction when the tumour is located in the posterior fossa (22).

Other intra-axial tumours at CPA include Medulloblastoma, Ependymoma and Hemangioblastoma which were not encountered in our study.

Medulloblastoma is a brain tumour of neuroepithelial origin, which represents 15-30% of a pediatric brain tumour and <1% of adult brain tumour. These are hypointense on T1WI and hyperintense on T2WI, it gives intense post contrast enhancement medulloblastoma can involve CPA in the extreme case of foramen extension usually in exophytic cerebellar mass. Ependymomas represent 3-9% of neuroepithelial neoplasm and, 6-12% of all pediatric tumours. The majority of intracranial ependymomas located in the posterior fossa, which arise from the floor of the fourth ventricle. Ependymomas are iso or hypointense on T1WI and hyperintense on T2WI with the specks of calcification and haemorrhage are commonly seen. It shows heterogeneous postcontrast enhancement. Ependymomas represent 3-9% of neuroepithelial neoplasm and, 6-12% of all pediatric tumours. The majority of intracranial ependymomas located in the posterior fossa, which arise from the floor of the fourth ventricle. Ependymomas are iso- or hypo-intense on T1WI and hyperintense on T2WI with the specks of calcification and haemorrhage are commonly seen. It shows heterogeneous postcontrast enhancement.

Skull base lesions

A few tumours arising from the skull base may extend, partially or extensively, in the CPA. Significant bony erosion associated with the mass lesion points toward the diagnosis of this type of lesion.

Paraganglioma

Most paragangliomas located in the CPA result from the extension of paragangliomas arising at the jugular foramen (glomus jugulare tumour) or in the middle ear (glomus tympanicum tumour). Indeed, only a few cases of primary paragangliomas originating from the CPA itself have been reported to date (22). These benign but locally aggressive tumours destroy the bones of the skull base with a moth-eaten erosion pattern at CT. At MRI, paragangliomas appear as highly vascular soft tissue lesions demonstrating a mix of multiple punctuate and serpentine signal voids corresponding to high-flow intratumoral vessels and foci of high-signal intensity due to intratumoral haemorrhages with methemoglobin, producing the characteristic salt-and-pepper appearance. A combination of unenhanced and contrast-enhanced 3D time-of-flight MR angiography has been proposed in addition to a standard imaging protocol to increase the detection of

these intratumoral vessels. Perfusion MR imaging demonstrates high vascularity patterns with high rCBV. Finally, conventional angiography shows an intense tumoral blush with enlarged feeding arteries, which may allow haemostatic embolisation before surgical resection, though it is rarely used as a primary diagnostic modality (22).

Chordoma

Intracranial chordomas are thought to originate from embryonic remnants of the primitive notochord and are located midline, near the clivus, from which they rarely extend into the CPA. Chondroid chordoma is a pathological subtype of chordoma that may have a more lateral origin in the petrous bone and grow directly in the CPA. All kinds of chordomas have, however, very similar imaging patterns, sometimes shared with chondrosarcomas as well, except that the latter usually have a more lateral origin. At CT, intracranial chordoma typically appears as a centrally located, well-circumscribed, expansile soft-tissue mass associated with extensive lytic destruction of the clivus. At MRI, on T1-weighted MR images, chordomas demonstrate intermediate to low signal intensity, with foci of T1 signal hyperintensity that may represent either residual ossified fragments of the skull base, tumour calcification, collections of proteinaceous fluid or haemorrhage (22). On T2-weighted MR images, they demonstrate the very high signal intensity and septa of low signal intensity that is considered characteristic. Slight enhancement is usually observed after contrast media administration.

Endolymphatic sac tumours

Endolymphatic sac tumours are aggressive papillary adenomatous tumours that originate from the endolymphatic sac, which is located at the posterior aspect of the petrous bone. These tumours may grow large enough to extend into the CPA and eventually compress the brain stem. Endolymphatic sac tumours occur sporadically or in the context of von Hippel-Lindau disease. Endolymphatic sac tumour is an extradural tumour that erodes and destroys the retrolabyrinthine petrous bone with geographic or moth-eaten margins at CT and may exhibit possible calcifications. At MRI, the lesion is heterogeneous on both T1- and T2-weighted images, with foci of high signal intensity due to intratumoral subacute haemorrhage. A T1- and T2-hyperintense cystic component, rich in blood and proteins may be present and is suggestive of the diagnosis in this very specific location. Notably, the cyst may be predominant and the mass itself can be almost entirely cystic in appearance in some cases (22). Finally, in masses larger than 2 cm in diameter, flow voids can be observed within and around these hypervascular tumours.

T1 high-signal-intensity lesions

An intrinsic T1 high-signal intensity of a non-enhancing CPA mass lesion favours a fatty or high protein content. T1-weighted sequence with fat signal suppression should then be performed in order to distinguish the exact nature of the high signal intensity: if it is suppressed, the tumour contains fat and is likely to be a lipoma or a dermoid cyst, if it is unchanged, the lesion has a high protein content and maybe a neurenteric cyst or a cholesterol granuloma.

Lipoma

Lipomas are benign lesions believed to result from abnormal differentiation of the primitive meninx. The majority of intracranial lipomas are located around the corpus callosum and about 100 cases have been reported in the CPA, where they encase normal adjacent neurovascular structures with very dense adhesions (22). Intracranial lipomas may be asymptomatic, incidentally discovered on brain imaging. They can also produce symptoms by compressing the adjacent cerebral structures, such as the cranial nerves in the CPA. At imaging, lipomas appear exactly the same as subcutaneous fat: homogeneously hypoattenuating on CT (except for possible superficial calcification) and with a homogeneous very high signal intensity on T1-weighted images, which decreases on fat-suppressed images, while no enhancement is observed after contrast administration.

Neurenteric cyst

Neurenteric cysts are congenital cystic masses lined by a mucin-producing epithelium of endodermal origin, closely resembling gastrointestinal tract mucosa. Intracranial neurenteric cysts are very unusual, mainly located near the midline in the posterior fossa or in the CPA. They present with round and smooth margins. The signal intensity of the cyst depends on its protein content. It can rarely mimic

CSF when this content is low, but it is often isointense to hyperintense relative to brain parenchyma on T1-weighted images and hyperintense on T2-weighted images when the protein concentration is high (22). Neurenteric cysts very rarely show peripheral rim enhancement. Differences exist in reports of the signal intensity on DWI and ADC values of the neurenteric cyst. However, based on the few cases of these cysts studied by DWI, it seems that the low signal intensity of neurenteric cysts on this sequence predominates. This imaging feature may enable differentiation from epidermoid cysts, which may exhibit similar intensities on conventional sequences but a characteristic high signal intensity on DWI.

Cholesterol granuloma

Cholesterol granulomas result from the chronic obstruction of air cells and the subsequent accumulation of their secretions. In the case of petrous apex origin, they can become large enough to expand in the CPA where they can compromise cranial nerves. They appear as expansile lytic lesions of the temporal bone with sharp and smooth margins, demonstrating a central region of high signal intensity and a peripheral hypointense rim on both T1- and T2-weighted images, the latter corresponding to the association of the expanded cortical bone and hemosiderin deposits. When desiccated, cholesterol granulomas can demonstrate areas of low signal intensity that give this homogeneous T1-hyperintense lesion and heterogeneous T2 pattern very suggestive of the diagnosis in this location (22). Cholesterol granuloma could be classified as a skull base lesion invading the CPA, but the usual lack of enhancement after contrast enhancement and its characteristic intrinsic T1-high signal intensity, make its classification in this category more relevant.

Non-enhancing lesions

T1 low-signal-intensity lesions

Epidermoid cyst

Epidermoid cysts are the congenital lesions arising from the accidental inclusion of ectodermal epithelial tissue during neural tube closure in the first weeks of embryogenesis. About half of intracranial epidermoid cysts are located in the cerebellopontine angle, where they represent 5% of overall lesions and the third most common mass behind vestibular schwannomas and meningiomas. Epidermoid cysts are lesions that grow from the slow desquamation of the stratified keratinised epithelium that lines the cyst. These malleable masses insinuate into posterior fossa cisterns, encasing cranial nerves and vessels with a specific irregular lobulated cauliflower-like outer surface (22). Because of the relative softness of epidermoid cysts and their tendency to include rather than displace adjacent structures, clinical symptoms occur only when the masses are large. At CT, epidermoid cysts appear hypoattenuating with possible marginal calcifications. At MRI, they have a fluid-like low T1 signal intensity and high T2 signal intensity, but they are slightly brighter than CSF on both T1- and T2-weighted images. They may, however, be difficult to distinguish from arachnoid cysts on these sequences, based on signal intensity alone. On FLAIR sequence, epidermoid cysts can be easily differentiated from arachnoid cysts because the former show mixed iso- to hyper signal intensities, but with poor demarcation, while the signal of the latter is suppressed, as the signal of CSF. MR cisternography, by means of heavily T2-weighted 3D sequence, demonstrates an epidermoid cyst signal hypointense to CSF, reveals the lobulated margins of the tumour, and clearly depicts the anatomical relation to nearby nerves and vessels and its precise extent for surgical planning. DWI offers a finding specific for extra-axial epidermoid cysts by showing a very high signal. Restricted ADC compared to CSF, almost comparable to that of the brain, and T2 shine-through effect both play an important role in the high signal intensity of epidermoid cyst at DWI. DWI is also crucial in the postoperative follow-up as it allows confirmation of the presence of a possible residual tumour. Finally, MR spectroscopy is also helpful as it shows only elevated lactate peaks in these tumours, which can be of interest in case of atypical epidermoid cysts. Indeed, in very limited cases, unusual patterns of epidermoid cysts may be observed on MRI. Such circumstances include so-called white epidermoids which have a rich protein content and appear with reversed signal intensities with homogeneous high signal intensity on T1-weighted images and low signal intensity on T2-weighted images, intracystic haemorrhage with heterogeneous signal intensities due to blood products or malignant transformation into squamous cell carcinoma which should be considered in case of frank contrast enhancement (22).

Arachnoid cyst

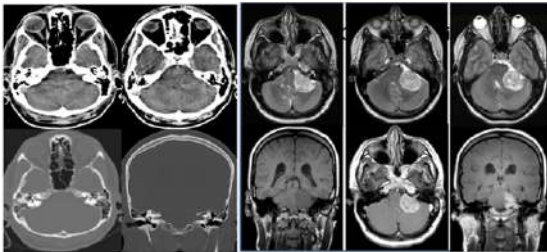
Arachnoid cysts are congenital, benign, intra-arachnoid pouch-like lesions filled with normal CSF. Their exact origin is uncertain, but they could result from a splitting of the embryonic meninges (22). They are usually supratentorial, with about 70% being in the temporal fossa, mostly on the left side, anterior to the temporal poles. Only 10% of arachnoid cysts are located in the posterior fossa, where they most commonly develop in the CPA. The large majority of arachnoid cysts are asymptomatic and found incidentally at imaging, but they can compromise cranial nerve functions in the posterior fossa by stretching them. Spontaneous or traumatic intracystic haemorrhage can also complicate arachnoid cysts, though this has only rarely been described in the posterior fossa. At neuroimaging, attenuation and signal intensities of uncomplicated arachnoid cysts exactly match those of CSF on all sequences, do not enhance after contrast media administration, and therefore, may mimic epidermoid cysts on conventional T1- and T2-weighted images. However, arachnoid cysts displace adjacent arteries and cranial nerves rather than encasing them, as epidermoid cysts usually do. They also demonstrate rounded edges, smoothly deforming the adjacent brain or scalloping the bony structures. Additionally, the complete suppression of signal intensity on FLAIR sequence in arachnoid cysts and the lack of diffusion restriction of these lesions on DWI should eliminate epidermoid cyst as a likely differential diagnosis of arachnoid cysts (22).

CONCLUSION

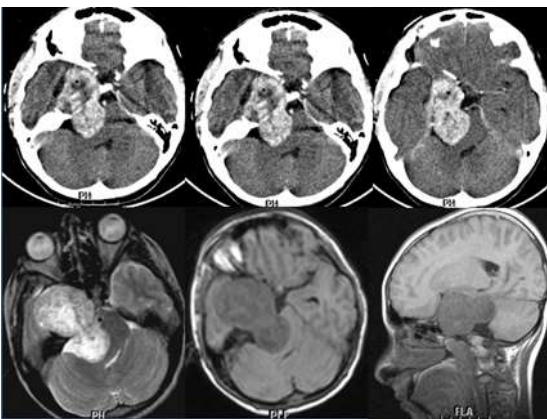
A wide variety of lesions can be encountered in the Cerebellopontine angle (CPA). A meticulous analysis of the site of origin, shape, density, signal intensities and behaviour after contrast media injection allows a systematic approach to the preoperative diagnosis in the majority of cases. Diffusion and perfusion-weighted imaging, as well as MR spectroscopy, may also provide crucial information that helps radiologists arrive at the correct diagnosis non-invasively.

REPRESENTATIVE CASES

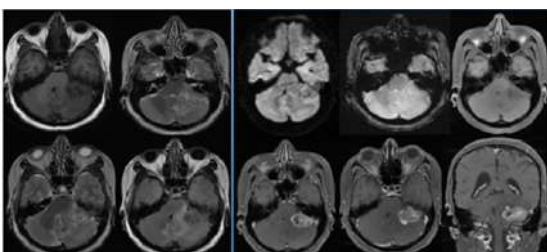
Case 1 CT & MRI Showing Case Of Left Vestibular Schwannoma



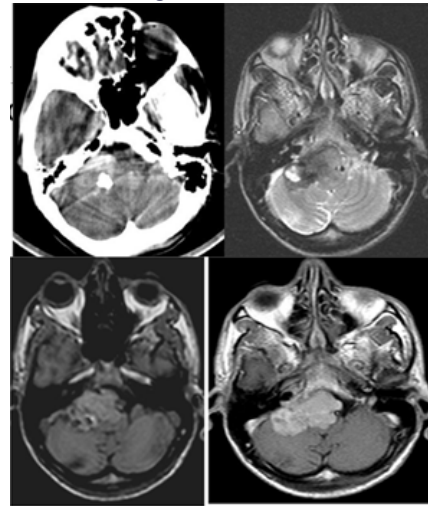
Case 2 CT & MRI Showing Case Of Meningioma



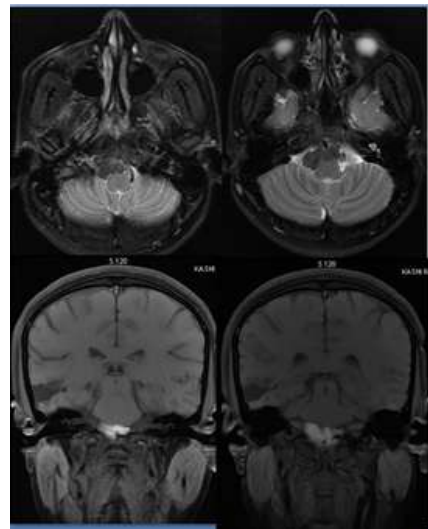
Case 3 MRI Showing Case Of Metastasis



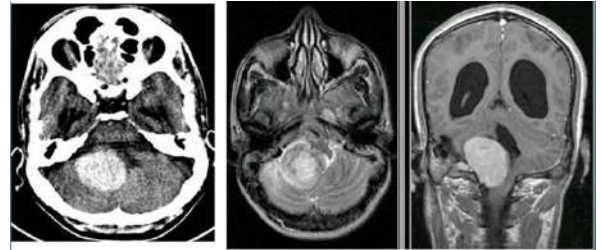
Case 4 CT & MRI Showing Case Of Melanoma



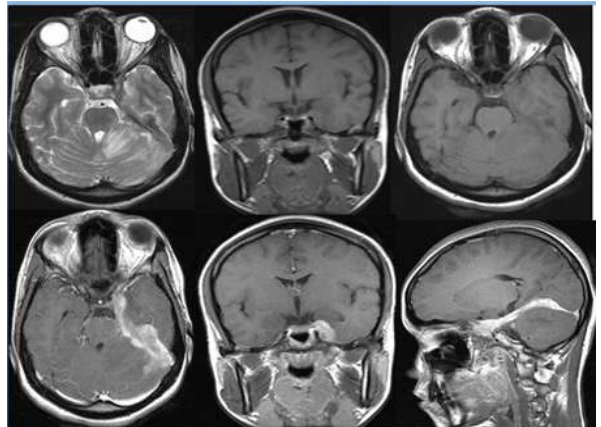
Case 5 MRI Showing Case Of White Epidermoid

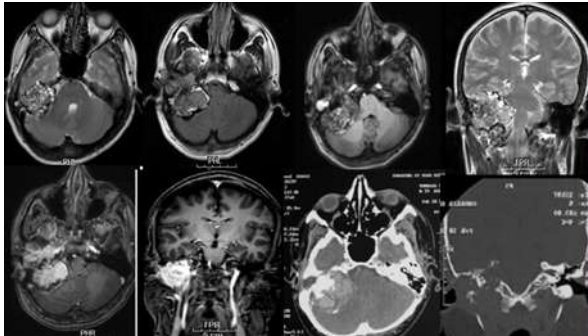
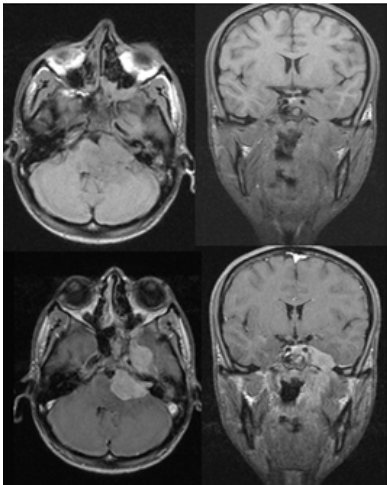
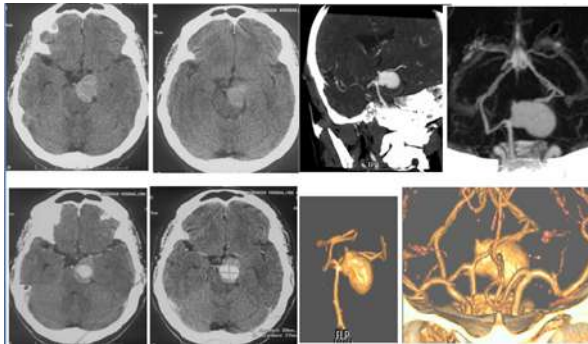


Case 6 CT & MRI Showing Case Of Pseudotumour



Case 7 MRI Showing Case Of Tuberculosis



Case 8 CT & MRI Showing Case Of Paraganglioma**Case 9 MRI Showing Case Of Perineural Spread Of Nasopharyngeal Carcinoma****Case 10 CT And CT Angiography Images Showing Case Of Basilar Artery Aneurysm****REFERENCES**

- Bailey BJ, Johnson JT, Shaw D. Head & Neck Surgery: Otolaryngology. Newlands: Lippincott Williams & Wilkins; 2006.
- Schaller B. Cerebellopontine angle surgery. Part 1: General remarks. HNO 2003;51:284-95.
- Brackmann DE, Kwartler JA. A review of acoustic tumors: 1983-1988. Am J Otol 1990;11:216-32.
- Smirniotopoulos JG, Yue NC, Rushing EJ. Cerebellopontine angle masses: Radiologic-pathologic correlation. Radiographics 1993;13:1131-47.
- Woodruff JM, Kourea HP, Louis DN. Tumors of cranial and peripheral nerves. In: Kleihues P, Cavenee WK, editors. Pathology and Genetics of Tumors of the Nervous System. Lyon: International Agency for Research on Cancer; 2000. p. 163-74.
- Bonneville F, Sarrazin JL, Dupuch KM, Ifeacker C, Cordoliani YS, Doyon D, Bonneville JF. Unusual Lesions of the Cerebellopontine Angle: A Segmental Approach. Radiographics 2001;21:419-38.
- Brunori A, Scarano P, Chiappetta F. Non-acoustic neuroma tumor (NANT) of the cerebello-pontine angle: A 15-year experience. J Neurosurg Sci 1997;41:159-68.
- Casadei GP, Komori T, Scheithauer BW, Miller GM, Parisi JE, Kelly PJ. Intracranial parenchymal schwannoma. A clinicopathological and neuroimaging study of nine cases. J Neurosurg 1993;79:217-22.
- Smirniotopoulos JG, editor. Extra axial masses of the central nervous system. In: Categorical Course in Diagnostic Radiology: Neuroradiology. Oak Brook, Ill: Radiological Society of North America; 2000. p. 123-32.
- Mulvihill JJ, Parry DM, Sherman JL, Pikus A, Kaiser-Kupfer MI, Eldridge R. NIH conference. Neurofibromatosis 1 (Recklinghausen disease) and neurofibromatosis 2 (bilateral acoustic neurofibromatosis). An update. Ann Intern Med 1990;113:39-52.
- Smirniotopoulos JG, Murphy FM. The phakomatoses. AJNR Am J Neuroradiol 1992;13:725-46.
- Ricci PE. Imaging of adult brain tumors. Neuroimaging ClinNAM 1999;9:651-69.
- Osborn AG, editor. Meningiomas and other nonglioma neoplasms. In: Diagnostic Neuroradiology. St. Louis: Mosby; 1994. p. 579-625.
- CBTRUS. Statistical Report: Primary Brain Tumors in the United States, 1998-2002. Central Brain Tumor Registry of the United States; 2005.
- Sarrazin JL. Infra tentorial tumors. J Radiol 2006;87(6 Pt 2):748-63.
- Woodruff JM, Kourea HP, Louis DN, Scheithauer BW. Tumours of cranial and peripheral nerves. In: Kleihues P, Cavenee WK, editors. Pathology and Genetics of Tumours of the Nervous System. Lyon: International Agency for Research on Cancer; 2000. p. 163-74.
- Commins DL, Atkinson RD, Burnett ME. Review of meningioma histopathology. Neurosurg Focus 2007;23:E3.
- Smith SJ, Boddu S, Macarthur DC. Atypical meningiomas: WHO moved the goalposts? Br J Neurosurg 2007;21:588-92.
- Willis J, Smith C, Ironside JW, Erridge S, Whittle IR, Everington D. The accuracy of meningioma grading: A 10-year retrospective audit. NeuropatholApplNeurobiol 2005;31:141-9.
- Atlas SW, Lavi E, Goldberg HI. Extra axial brain tumors. In: Atlas SW, editor. Magnetic Resonance Imaging of the Brain and Spine. 3rd ed. Philadelphia: Lippincott Williams & Wilkins; 2002. p. 695-772.
- New PF, Hesselink JR, O'Carroll CP, Kleinman GM. Malignant meningiomas: CT and histologic criteria, including a new CT sign. AJNR Am J Neuroradiol 1982;3:267-76.
- Fabrice Bonneville Julien Savatovsky Jacques ChirasEurRadiol (2007) 17: 2908–2920 DOI 10.1007/s00330-007-0680-4
- Bertrand RA, Molina P, Hardy J. Vestibular syndrome and vascular anomaly in the cerebello-pontine angle. Acta Otolaryngol 1977;83:187-94.
- Hofmann E, Behr R, Neumann-Haefelin T, Schwager K. Pulsatile tinnitus: Imaging and differential diagnosis. DtschArztblInt 2013;110:451-8.
- Wuertenberger CJ, Rosahl SK. Vertigo and tinnitus caused by vascular compression of the vestibulocochlear nerve, not intracanalicular vestibular schwannoma: Review and case presentation. Skull Base 2009;19:417-24.
- Fabrice Bonneville Julien Savatovsky Jacques ChirasEurRadiol (2007) 17: 2472–2482 DOI 10.1007/s00330-007-0679-x